Title

Optimization of a Biomimetic Apatite Nanoparticle Delivery System for Non-viral Gene Transfection - a Simulated Body Fluid Approach

Author

Das, Debobrato

Publication Date

2013

Peer reviewed|Thesis/dissertation

UNIVERISITY OF CALIFORNIA

Los Angeles

Optimization of a Biomimetic Apatite Nanoparticle Delivery System for Non-viral Gene Transfection – a Simulated Body Fluid Approach

A thesis submitted in partial satisfaction of the requirements for the degree Master of Science in Bioengineering

by

Deobobrato Das

2013

ABSTRACT OF THE THESIS

Optimization of a Biomimetic Apatite Nanoparticle

Delivery System for Non-viral

Gene Transfection – a Simulated Body Fluid Approach

by

Debobrato Das

Master of Science in Bioengineering

University of California, Los Angeles, 2013

Professor Benjamin M. Wu, Chair

Current methods for gene delivery utilize nanocarriers such as liposomes and viral vectors that may produce *in vivo* toxicity, immunogenicity, or mutagenesis. Moreover, these common high-cost systems have a low efficacy of gene-vehicle transport across the cell plasma membrane followed by inadequate release and weak intracellular stability of the genetic sequence. Thus, this study aims to maximize gene transfection while minimizing cytotoxicity by utilizing supersaturated blood-plasma ions derived from simulated body fluids (SBF).

With favorable electrostatic interactions to create biocompatible calcium-phosphate nanoparticles (NPs) derived from biomimetic apatite (BA), results suggest that the SBF system, though naturally sensitive to reaction conditions, after optimization can serve as a tunable and versatile platform for the delivery of various types of nucleic acids. From a systematic exploration of the effects of nucleation pH, incubation temperature, and time on transfection efficiency, the study proposes distinct characteristic trends in SBF BA-NP morphology, cellular uptake, cell viability, and gene modulation. Specifically, with aggressive nucleation and growth of BA-NPs in solution (observed via scanning electron microscopy), the ensuing microenvironment imposes a more toxic cellular interaction (indicated by alamarBlue and BCA assays), limiting particle uptake (fluorescence experiments) and subsequent gene knockdown (quantitative loss of function assays). Controlled precipitation of BA-NPs function to increase particle accessibility by surrounding cells, and subsequently enhance uptake and transfection efficiency. By closely examining such trends, an optimal fabrication condition of pH 6.5-37C can be observed where particle growth is more tamed and less chaotic, providing improved, favorable cellular interactions that increase cell uptake and consequently maximize gene transfection, without compromising cellular viability.

The thesis of Debobrato Das is approved.

Min Lee

Daniel T. Kamei

Benjamin M. Wu, Committee Chair

University of California, Los Angeles

2013

TABLE OF CONTENTS

LIST OF FIGURES

LIST OF TABLES

LIST OF ACRONYMS

Simulated Body Fluid (SBF)

Nanoparticle/s (NP/s)

Biomimetic Apatite (BA)

Bicinchoninic Acid Assay (BCA)

RNA interference (RNAi)

Plasmid DNA (pDNA)

Calcium-phosphate (CaP)

Small interfering RNA (siRNA)

microRNA (miRNA)

Scanning electron microscopy (SEM)

Glyceraldehyde 3-phosphate dehydrogenase (GAPDH)

Phosphate buffer solution (PBS)

Protein tyrosine kinase-9 (PTK-9)

4’,6-diamidino-2-phenylindole (DAPI)

Fluorescein isothiocyanate (FITC)

Fluorescein amidite (FAM)

ACKNOWLEDGEMENTS

The author would like to gratefully acknowledge Dr. Benjmain Wu, Dr. Patricia Zuk, and Eric Tsang for their valuable mentorship and scientific support in this project.

1. INTRODUCTION

Gene therapy is commonly used to amplify functions of missing or defective genes and silence disease causing genes using antisense therapy or RNA interference (RNAi) pathways. Understanding and developing creative, non-toxic platforms to encapsulate and deliver such genetic vectors serve as means to increase the efficacy of this directed intracellular therapy. High-costing viral vectors, though known to be quite efficient, have significant disadvantages (*i.e.* limited nucleic acid carrying capacity, promoting mutagenesis) and can impose safety concerns for a system, from immunogenicity to toxicity [1-3]. Thus non-viral vectors are being investigated to address these shortcomings and provide a reliable, yet safer and more cost efficient mode for gene therapy [4, 5].

Conventional methods for non-viral mediated gene delivery utilize cationic liposomes, polymers, and peptides that may vary in transfection efficiency and toxicity due to inactivation by serum proteins, limited cellular uptake, improper endosomal release, and weak intracellular stability of resulting transgene [2, 6]. Cationic lipids, a contemporary vector platform, are composed of amphiphilic domains that can provide colloidal stability in solution mediated by structural variations of the hydrophilic lipid head group (*i.e.* size and charge) and hydrophobic alkyl chains (*i.e.* length and degree of saturations) [7, 8]. Mechanistically, spontaneous DNA/RNAi association with cationic lipid vectors are formed by electrostatic interactions between positively charged head groups of the lipid and negatively charged phosphate backbone of the nucleic acid. In order to achieve adequate compaction of these negatively charged nucleic acids, often times a lipid with greater positive charge at physiological conditions is employed, resulting in appropriate cargo encapsulation [9, 10]. Moreover, lipid-DNA/RNAi complexes that have an overall net positive charge can also be used to target negatively charged membranes of

cells to allow for internalization [6-8]. This approach, thus, offers highly efficient transfection of desired genes to certain cell types and is known to complex a wide variety of nucleic acids varying in sizes. However, cationic lipid systems, in addition to not being able to deliver to all cell types, tend to provide enhanced cytotoxicity due to the surplus positive charge [8-10].

Highly cationic polymer systems, such as DEAE-dextran, have been historically used to complex negatively charged nucleic acids and target plasma membranes of cells similar to cationic lipids [11]. Nevertheless, unlike lipids, these polymers customarily exclude hydrophobic domains, and are consequently completely water soluble. Furthermore, these polymers can be synthesized into various architectures (*i.e.* linear or branched) with customized charge distribution that can result in more efficient compaction and condensing of DNA [8, 9]. More specifically, dendrimers (*i.e.* polyamidoamine) are a familiar polymer structure used by many, which have surface residing positive amino groups that interact through electrostatics with negatively charged DNA [11, 12]. A valued utility of such polymeric morphologies stems from the presence of deprotonated amino groups at physiological pH, and the highly condensed nature of the nucleic acid upon endosomal internalization and trafficking [12, 13]. The local acidic microenvironment of the endosome causes protonation of amino groups, which aids to buffer and inhibit DNA degradation by pH-dependent endosomal nucleases. Though the incorporation of DEAE-dextran, for example, can be fairly inexpensive and applicable to a wide range of cell types, high concentrations of such positively charged polymers results in increased toxicities to cells [13-15]. Furthermore, studies have shown from utilizing DEAE-dextran systems, transfection efficiencies can vary from high-to-low depending on cell type, and in general, this approach is more suitable for transient transfection strategies rather than long-term, stable transfection where the DNA cargo integrates with host chromosome [12, 14].

Physical methods for transfection, though not as common as chemical vehicles, can provide a more natural substitute for gene delivery [7]. For example, electroporation, initially described as means to transfect genes in mouse cells, utilizes electrical pulse-trains to agitate cell membranes and subsequently generate transitory pores to transport genes [9]. This approach, while efficient under certain optimized conditions, can result in high cell death and can be costly to perform and maintain [8]. In addition, physical microinjection single-cell techniques can be used on a variety of cell types with high accuracy; however, this process can be expensive and labor intensive requiring technical expertise [16].

Amongst the various systems used for non-viral gene delivery, calcium-phosphate (CaP) nanocarriers have received much attention due to their relative success in gene therapy *in vitro*. CaP based platforms offer a low-cost, highly efficient transfection strategy that is applicable to diverse cell types, and can be exploited for both long-term and transient gene modulation studies [17]. The method was first investigated as an alternative to the DEAE-dextran approach for DNA transfection and was soon after implemented to deliver plasmid DNA (pDNA) as means for gene modulation [1, 18]. Fundamentally, these CaP constructs arise from mixing negatively charged nucleic acids with calcium chloride to create precipitates that can be buffered by the addition of phosphate ions. Currently, there exist multiple approaches for formulating CaP-RNAi/DNA nanocomplexes, from co-precipitation [4, 19] to encapsulation [1, 20] to formation of multi-shell structures [21-23], each varying in synthesizing conditions and techniques that result in unique nanocarrier attributes. Both co-precipitation of small nucleic acids (*i.e.* RNAi) with CaP and encapsulation of pDNA by CaP clusters, creates desirable complexes in supersaturated solutions, while multi-shell structures, though advantageous for larger cargo (*i.e.* oligonucleotides), requires harsher reaction conditions in order to maintain colloidal stability [17, 22].

As recognized by previous investigators, CaP-RNAi/DNA nanoparticles (NPs) are internalized by target cells through an endocytic pathway that allows for dissociation of the particle in the more acidic microenvironment of the endosomal vessel [3, 18]. More specifically, the kinetics of NP disassembly within the endosome is mediated by electrostatic interactions between the slight positively charged inner vessel-wall and the negatively charged ionic species of the NP [3]. The resulting RNAi/DNA genetic sequence(s) are presented to the cytoplasm where they can achieve bioactivity.

Simulated body fluid (SBF), composed from concentrated version of native blood plasma ions, was originally utilized to understand surface morphology of biomimetic ceramics [24, 25], and has since been popularly exploited to study CaP (biomimetic-apatite) precipitation and growth on surfaces of biomaterials as means to predict *in vivo* bone bioactivity [26-28]. The rationale behind employing apatite into design models for materials and implants stems from the notion that native bone binding, interaction, and incorporation can be favorably governed by fabricating bone-like apatite layers on bone-material interfaces [29, 30]. Essentially, the nucleation and growth of such apatite is a dynamic process dependent on consumable CaP found in SBF. Biomimetic apatite (BA) coatings have subsequently been used to coat implants and biodegradable scaffolds due to the favorable biocompatibility that exists with CaP based systems [6, 31]. Thus, CaP-NPs derived from SBF-BA can allow for an attractive gene delivery platform as non-viral vectors due to their low production cost, known biodegradability profiles, and enhanced cellular viability compared to traditional non-viral methods. Unlike traditionally fabricated CaP-NPs (from the simple mixture of calcium chloride, pDNA/RNAi, and phosphate ions) where precipitate growth is more random providing large particle aggregates, utilizing SBF can serve to better control the nucleation of these particles by the presence of *various* buffering

ions, and thereby increase the overall efficacy for gene therapy of the CaP-NP platform [17, 27]. In addition, CaP-NPs have been shown to transfect a wide range of cell lines, while still maintaining biocompatibility and therapeutic efficacy of transgenes [32].

However, the fabrication of SBF-BA in general and SBF BA-NPs in particular are innately quite sensitive to reaction conditions [24, 33-35] and despite all the attention of using this system for gene delivery, there has relatively been few studies that have looked at the optimization of this process and consequently the effects of varying synthesizing parameters on gene transfection and modulation. Instead, there specifically seems to be a diverse array of synthesizing conditions proposed to produce ideal environments necessary to create well complexed crystals or particles for applications in coating of biomaterials [36-40]. Three of the main parameters in BA-NP synthesis are nucleation pH, temperature, and time with investigators reporting diverse effective conditions. By having a better understanding of the regulatory cues present in the SBF microenvironment, synthesis of BA-NP can be more precisely controlled for adaptable gene delivery and allow for highly reproducible results. Moreover, the majority of literature has investigated the transfection of these non-viral vectors using pDNA to multiple cell lines (*i.e.* HEK 293T or MLC-6 cells) [32], yet little has been explored about the incorporation of different types of nucleic acids (*i.e.* siRNA and miRNA) while using the same formulations of SBF. Therefore, by manipulating a previously established protocol for creating SBF derived particles, the goal of this study is to (i) systematically analyze the effects of key tunable parameters on BA-NP fabrication, cellular uptake, cytotoxicity, and transfection efficiency, and (ii) attempt to elucidate to an optimized reaction condition that maximizes gene modulation without compromising cellular viability, while creating a versatile platform for the delivery of various RNAi sequences.

2. MATERIALS AND METHODS

2.1 Materials Preparation

2.1.1 Concentrated simulated body fluid (SBF) preparation

BA-NPs, stabilized by ionic interactions between CaP, were constructed from SBF, which have historically been used to create apatite coatings that elicit *in vivo* bone bioactivity and decrease immunogenicity. SBF solutions were prepared (Fig. 1a) by sequentially dissolving $CaCl_2$, $MgCl_2 \cdot 6H_2O$, $NaHCO_3$, and $K_2HPO_4 \cdot 3H_2O$ (Table 1) in distilled deionized water resulting in an opaque white mixture [24]. The pH of the mixture was gradually lowered to 6 by adding concentrated HCl in small and controlled amounts to make the solution clear and increase solubility. Na_2SO^4, KCl, and NaCl (Table 1) were then added as the remaining components (buffers) of the SBF solution [25], and the pH was then raised using combinations of diluted NaOH and HCl to a final nucleation pH of 5.8, 6.5, or 7.4 depending on desired reaction conditions. Resulting solutions were sterilized using a tube-top vacuum filter system consisting of a 0.22 µm cellulose acetate membrane (Corning®, CA). All reagents were acquired from Sigma-Aldrich.

Ion conc. (mM)	Na^+	K^+	Ca^{2+}	Mg^{2+}	HCO_3^-	Cl^-	HPO_4^{2-}	SO_4^{2-}
Blood Plasma	142	5	2.5	1.5	27	103	1	0.5
SBF (5X)	710	25	12.5	7.5	21	740	5	2.5

Table 1. ***Ionic compositions of supersaturated SBF solution derived from native blood plasma***

2.1.2 Synthesis of biomimetic apatite nanoparticles (BA-NPs)

To initiate nucleation and growth of NPs, 50 µL of filtered SBF solutions of appropriate final pH comprised of amorphous CaP clusters (Fig. 1b) were homogenously mixed with 2 µL of

RNAi (Fig. 1c) by slowly pipetting up and down into centrifuge tubes. The resulting SBF-RNAi solutions were left to incubate in waterbaths at three different temperatures (25°C, 37°C, and 45°C) and varying times (10 min, 20 min, and 30 min). After incubation, BA-NP samples (Fig. 1d) from each tube were collected and assessed for materials properties or delivered to cells for uptake (Fig. 1e-g), measurements of viability, and gene modulation (Fig. 1h-i).

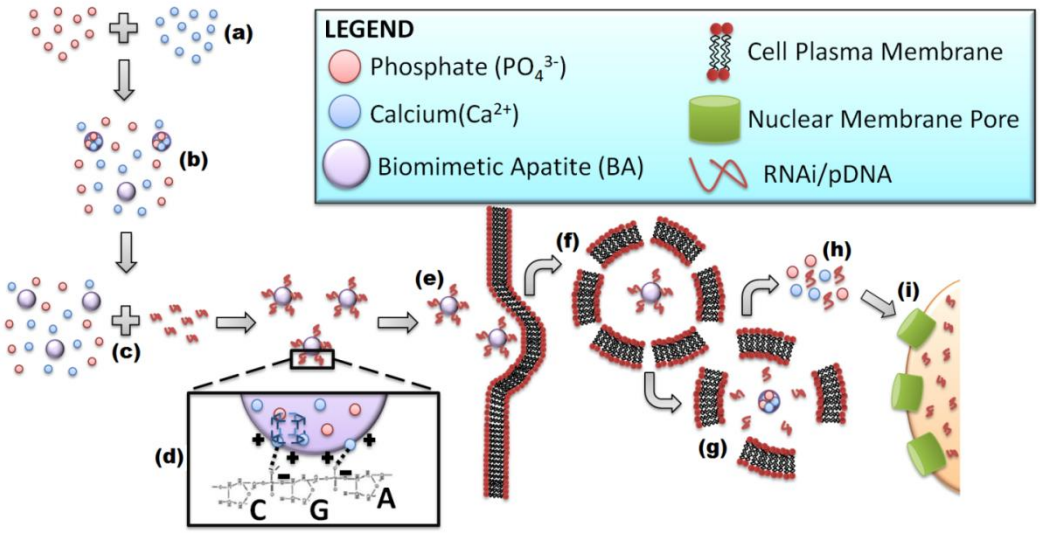

FIGURE 1. Formation of SBF BA-RNAi/pDNA and mechanism of action. This is a general schematic representation of the fabrication and subsequent application of SBF BA-NP systems for gene transfection. Initially, SBF solution is prepared (a) from concentrated version of native blood plasma ions added sequentially in a pH and temperature controlled microenvironment to create amorphous CaP clusters (b). These spherical clusters are mixed with desired RNAi/pDNA sequences (c) under appropriate reaction conditions. The resulting CaP-RNAi/pDNA NPs, composed of hexagonal-closed packed apatite based lattice-microarchitectures (shown with dotted line), are stabilized by electrostatic interactions (d) between positive Ca^{2+} residues and negatively charged backbone of nucleic acids. After fabrication, the SBF BA-NPs are administered to cells (e), and allowed to undergo endocytic internalization across plasma membrane (f). Consequently, endosomal breakdown occurs (g) as local pH levels drop, and CaP ions disassociate releasing the entrapped RNAi/pDNA (h). The naked RNAi/pDNA sequences are free to migrate within the cell, and depending on the type of genetic material, can potentially be delivered into the nucleus (i) for direct gene therapy

2.2 Materials Characterization

2.2.1 Scanning Electron Microscopy

SBF BA-NP samples, after proper incubation, were centrifuged at 4°C and 14,000 rotations per minute for 15 minutes. The samples were then collected, supernatants aspirated, and the remaining BA-NP solutions were resuspended in 50 µL of ultrapure water. This process was

repeated an additional time to ensure that the NP samples were dilute enough to allow for proper visualization under scanning electron microscopy. Lastly, 2 µL of final CaP solutions were allocated on carbon coated SEM stubs and allowed to air-dry overnight. The apatite NPs were imaged with a field emission SEM (Phillips/FEI XL-30) for different synthesis conditions at low and high magnifications to understand changes in BA-NP morphologies.

2.3 Cell-NP Interaction

2.3.1 Cell Culture

MC3T3-E1 cells, a commonly used (model) osteoblastic cell line derived from mouse calvaria to investigate bone biology, were grown in 75-cm^2 tissue culture flasks in the presence of Dulbecco's modified Eagle's medium (DMEM, Gibco) supplemented with 10% fetal bovine serum (FBS) and 1% penicillin-streptomycin. Cells of approximately 70-80% confluence were subsequently used to examine cell uptake, cytotoxicity, and gene regulation.

2.3.2 Cellular uptake of SBF BA-RNAi NPs

MC3T3 cells, seeded at 20,000 cells per well on 8 well-chambered culture slides, were administered fluorescently labeled BA-siRNA-FITC or BA-miRNA-FAM NPs (Fig. 1e) and allowed to be incubated at 37C with 5% CO_2 in serum-free Alpha Modification of Eagle's Medium (AMEM, Gibco). After 4h, culture medium was changed to original DMEM with serum before qualitative fluorescence images were acquired 24h post transfection. Cells were gently washed with phosphate buffer solution (PBS) and fixed using 4% paraformaldehyde before adding DAPI histology mounting medium (Sigma-Aldrich). All uptake studies were carried out under minimal light exposure to reduce photobleaching.

The effects of cell uptake were considered for various SBF BA-RNAi NP preparation conditions and against Lipofectamine® (Invitrogen, CA), a traditional transfection reagent made up of polycationic and neutral lipid molecules in membrane filtered water. Lipofectamine® controls were prepared according to manufacturer's guidelines. Fluorescently labeled RNAi were acquired from Invitrogen.

2.3.3 Colocalization of SBF BA-RNAi NPs

Colocalization assays using LysoTracker® Red (Life Technologies, CA) were conducted to examine endosomal trafficking of BA-RNAi NPs (Fig. 1f) as means to demonstrate mechanism of internalization.

2.3.4 Cytotoxicity of SBF BA-NP platform

Quantitative cellular viability of this SBF BA-NP system was evaluated using alamarBlue® and BCA assays for varied preparation parameters, including multiple NP concentrations, and compared against conventional Lipofectamine® formulations. Values were normalized to no-treatment conditions.

2.3.5 Gene modulation using SBF BA-RNAi NPs

To determine relative gene expression and consequently effective transfection (Fig. 1h-i), loss-of-function experiments exploiting common house-hold vector sequences of RNAi (*i.e.* GAPDH-siRNA and Pre-miR hsa-miR-1 miRNA from Life Technologies, CA) along with appropriate negative controls were conducted on SBF BA-NPs and Lipofectamine® based platforms. MC3T3 cells, seeded at 20,000 cells per well on tissue-culture treated polystyrene 24-

well cell culture plates, were administered SBF-BA and Lipofectamine -GAPDH siRNA or -hsa miRNA particles for 4h in the presence of serum free AMEM. Medium was altered to DMEM with serum after elapsed time, while final measurements of protein expression were conducted 48h post transfection.

For gene modulation using GAPDH siRNA, a horseradish peroxidase mediator was used to measure Glyceraldehyde 3-phosphate dehydrogenase (GAPDH) enzyme activity, which was indicated by a mean increase in fluorescence over time using a Tecan Microplate Reader at 590nm wavelength. Western Blot analyses with secondary (goat anti-mouse) antibodies specific to actin were performed on cells treated with -hsa miRNA to quantify protein tyrosine kinase-9 (PTK-9) activity, an enzyme responsible for tyrosine phosphorylation of actin. Upon proper initiation, both -GAPDH siRNA and -hsa miRNA function to down-regulate target enzyme activity, resulting in decreased expression of GAPDH and PTK-9, respectively.

2.4 Statistical Analysis

All data is illustrated as lower-upper limit %, indicating a relative range of percentages to normalized values. Cell viability (n=3) and gene modulation using -GAPDH siRNA (n=3) and -hsa miRNA (n=3) for each nucleation pH, temperature and time combinations were averaged and analyzed using two-way Analysis of Variance (ANOVA), while quantitative comparisons to Lipofectamine® were evaluated for significance using unpaired Student's t-test. A value of $p<0.05$ was used to determine statistical significance.

3. RESULTS

3.1 SBF BA-NP Morphological Qualities

SEM analysis at both 50,000x (not shown) and 100,00x was carried out at multiple nucleation pH, incubation temperature, and time to understand particle morphological properties. At higher temperatures (Fig. 2a), NP growth and nucleation is observed to be more clustered, resulting in large particle aggregates that are more often than not centered around prominent in situ forming salt crystals (white).

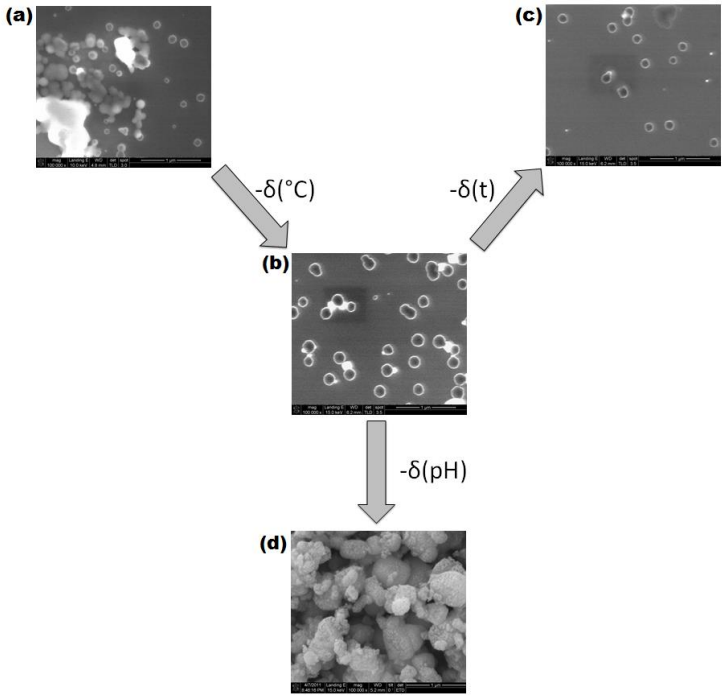

FIGURE 2. Scanning electron microscopy of SBF BA-siRNA NP solutions (100,000x). At pH 6.5-45C-30 min (a) NPs formed large clusters surrounded by aggressive salt crystal agglomerates. Decreasing incubation temperature (-δ°C) such that at pH 6.5-37C-30 min (b), allows for greater control over nucleation and growth of NP clusters and adjacent salt crystal precipitates. Modifying incubation time (-δt) from 30 min to 10 min at pH 6.5-37C (c) seems to limit the number of particles and salt crystals generated in solution, depicting a less saturated microenvironment compared to (a-b). Altering nucleation pH (-δpH) from 6.5 to pH 5.8-37C-30 min (d) produces a more chaotic microenvironment where particles and salt crystals of different size, shape, and morphology are created in a randomized fashion

Decreasing the temperature (-δ°C) seems to cause less particle aggregation as the growth and nucleation of these NPs are more controlled (Fig. 2b). Systematically reducing particle

incubation time (-δt) suggests impeded nucleation, as quantity and size of NPs decreases (Fig. 2c). Moreover, the size of remaining salt crystals appears to be consequently much smaller and the final NPs seem to be less clustered around salt-composed bodies. Decreasing nucleation pH (-δpH) seems to cause randomized growth of particles with different size and shape and tends to rapidly saturate the microenvironment (Fig. 2d). The resulting dominant salt crystals appear to also mimic native surrounding particle nature, having large robust domains, implying that the development of SBF lattice salt structures might be influenced simultaneously with SBF NP morphologies by varying similar tunable reaction parameters.

3.2 Cellular Uptake Using SBF BA-NPs

Particles of different synthesizing conditions were loaded with siRNA-FITC and used to assess uptake in MC3T3-E1 cells. Images from confocal microscopy were acquired at varying time points from multiple temperatures and nucleation pH. Initially increasing incubation time from 10-30 min seems to gradually increase cell uptake, as indicated by slight increases in fluorescence localized to marked cells (Fig. 3a-c). At a constant nucleation pH and incubation time, increasing incubation temperature seems to have a larger visible effect on cell uptake than incubation time alone. More specifically, for both pH 5.8 (Fig. 3d-f) and pH 7.4 (Fig. 3g-i) at an incubation time of 30 min, the relative fluorescence seems to significantly increase from 25C-37C and noticeably decrease or remain the same from 37C-45C, implying that there exists a peak temperature around 37C independent of nucleation pH where cell uptake is maximized. For a given incubation temperature of 37C and incubation time of 30 min, there appears to exist negligible changes in fluorescence between pH 5.8 (Fig. 3e) and pH 7.4 (Fig. 3h). However, upon comparing cell uptake between pH 6.5 at 37C and 30 min (Fig. 3c) to pH 5.8 (Fig. 3e) and

pH 7.4 (Fig. 3h) at the same synthesizing conditions, there appears to be more distinct fluorescence signals emerging from definite cellular locations at pH 6.5 (Fig. 3c) than pH 5.8 (Fig. 3e) or pH 7.4 (Fig. 3h). Moreover, the presence of more cells at pH 5.8 (Fig. 3e) and pH 7.4 (Fig. 3h) at 37C and 30 min may act to mask the actual fluorescence experienced on a per cell basis; there is less number of BA-siRNA-FITC NPs transfecting a given cell at the aforementioned pH but since there seems to be larger number of cells present, the net fluorescence may remain artificially high.

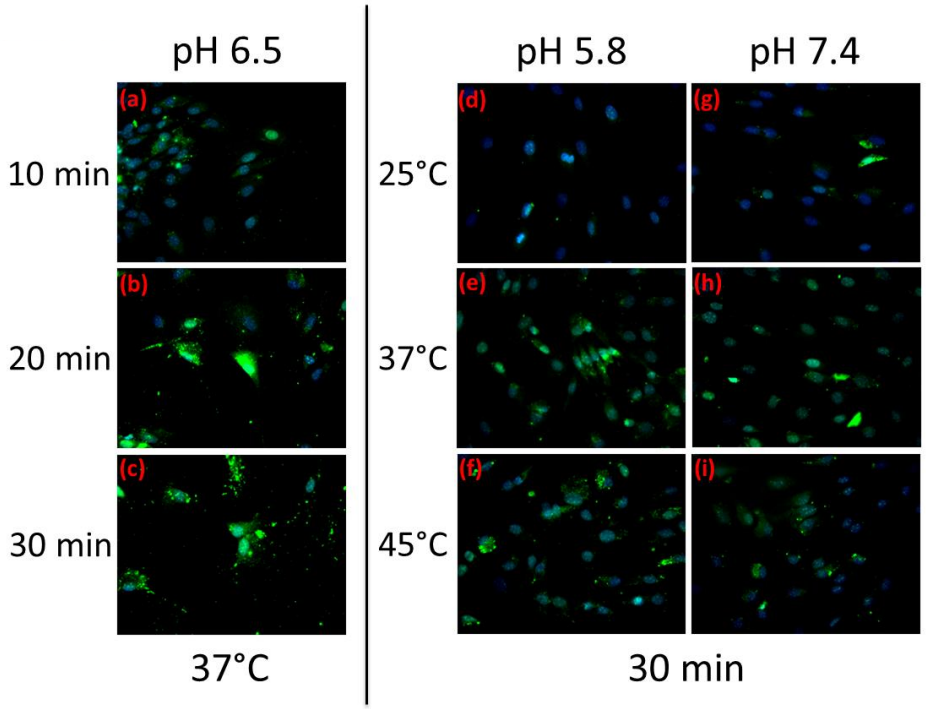

FIGURE 3. Uptake of SBF BA-siRNA-FITC NPs by MC3T3 cells. SBF BA-NPs containing fluorescently labeled siRNA were manufactured under different reaction parameters and sampled under confocal microscopy. At pH 6.5-37C, increasing incubation time from 10-30 min (a-c) seems to only minimally increase cell uptake, as marked by slight increases in distinct fluorescence with changes in time. Utilizing particles synthesized at pH 5.8-30 min as a function of increasing incubation temperature (d-f), cell uptake increases from 25C-37C but remains unchanged or slightly decreases from 37C-45C. A similar observation can be made for pH 7.4 (g-i) where there is a non-linear increase in overall fluorescence with increase in temperature. Comparing uptake at 37C-30 min for pH 6.5 (c) with pH 5.8 (e), and pH 7.4 (h), there appears to be greater discrete fluorescent signals emerging from pH 6.5 than pH 5.8 or 7.4, the latter of both producing more nuclear and widely dispersed signals, possibly arising from the presence of larger number of remaining cells

3.3 Colocalization of SBF BA-NPs

Images suggest that internalization of SBF BA-siRNA-FITC NPs seems to colocalize with endosomes and lysosomes, implying that trafficking of these particles involves endocytic vesicle compartmentalization, a mechanism that is also dominant when using other formulations of BA-RNAi. Specifically, this colocalization is indicated by the qualitative overlap of siRNA-FITC (green; Fig. 4a) with labeled endosomes or lysosomes (red; Fig. 4b), resulting in hints of yellow to symbolize union (Fig. 4c). Moreover, purple shades (Fig. 4c) originate in areas where both NPs loaded with siRNA-FITC and endosomes/lysosomes converge around the DAPI stained nucleus (blue).

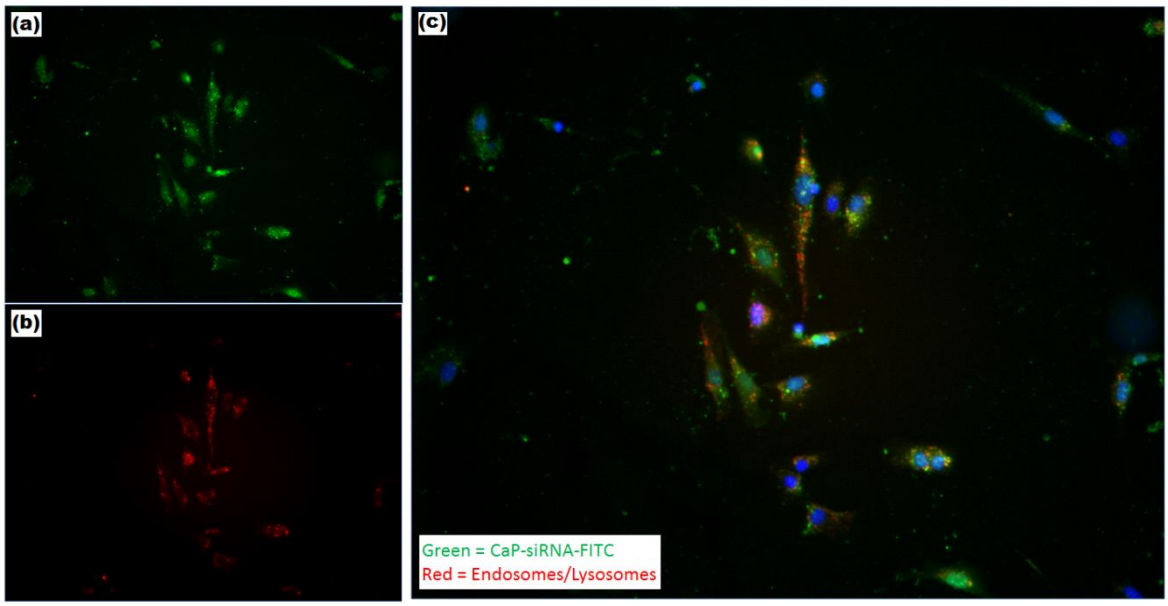

FIGURE 4. Colocalization of SBF BA-siRNA-FITC particles with endosomal vesicles. Green-fluorescently labeled siRNA entrapped within SBF BA-NPs (a) along with red-fluorescently labeled endosomes/lysosomes (b) are overlapped (c) to demonstrate common domains (shown as yellow or purple) to indicate an endocytic trafficking pathway, and subsequently help validate initially proposed mechanism of action for particle internalization

3.4 Cytotoxicity of SBF BA-NPs

alamarBlue® assays were utilized to examine cellular viability at various incubation temperatures and nucleation pH at both 10 min and 30 min time limits. Experimental conditions

were also compared against Lipofectamine®, a gold-standard transfection reagent utilized in many gene delivery studies. Moreover, relative percent values for viability were generated by normalizing data to no treatment conditions.

Data seems to suggest that independent of temperature and pH, increase in incubation time from 10 min to 30 min (Fig. 5a-c) has statistically negligible effect on cell viability. Furthermore, for a specified nucleation pH, increase in incubation temperature increases cytotoxicity as cell viability decreases. For example, at pH 5.8 (Fig. 5a) the relative percent viability is around 88-90% for 25C, while for 45C viability drops to around 60-65%. Focusing on a given incubation temperature, an increase in nucleation pH from 5.8 (Fig. 5a) to pH 7.4 (Fig. 5c) may seem to *initially* provide similar cytotoxicities.

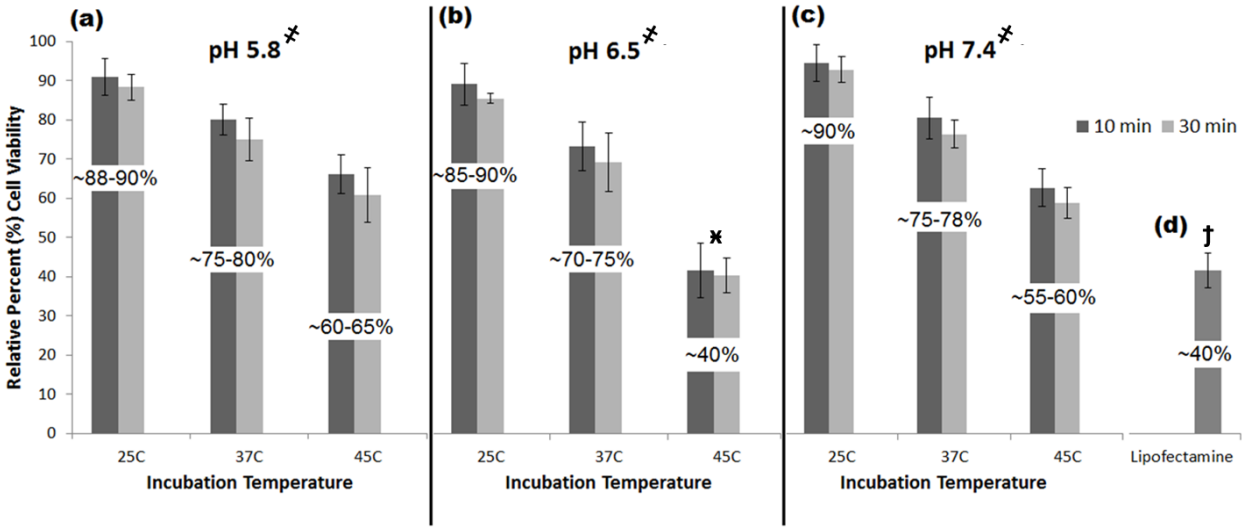

FIGURE 5. MC3T3 cell viability in the presence of SBF BA-siRNA NPs. Independent of nucleation pH and incubation temperature, increasing the incubation time from 10-30 min produces statistically insignificant changes in percent cell viabilities (a-c). Moreover, for a given pH, an increase in incubation temperature, in general, increases cytotoxicity or decreases cell viabilities (a-c). However, specifically, cell viabilities for a given incubation temperature tend to be greater at pH 5.8 (a) and pH 7.4 (c) than pH 6.5 (b). In fact, an increase in temperature results in larger increase in cytotoxicities at pH 6.5 (c). Comparing the SBF system to Lipofectamine® (d), it seems that only particles generated at pH 6.5-45C (b) produces the same order of magnitude of toxicity (~40%) as the liposomal carrier, whereas remaining reaction conditions promote particles with statistically greater percent viabilities. *Statistical significance maintained: ≠between nucleation pH ($p<0.042$); ×among incubation temperature ($p<0.033$); †compared to most reaction conditions with the exception of pH 6.5-45C-30 min ($p<0.027$)*

Specifically, for an incubation temperature as low as 25C, a raise in nucleation pH maintains original viabilities at ~85-90% (Fig. 5b). However, at higher temperatures of 37C, this

trend seems to deviate as viability remains higher at pH 5.8 (Fig. 5a) and pH 7.4 (Fig. 5c), but decreases at pH 6.5 (Fig. 5b) to ~70-75%. Additionally, this emerging division in cytotoxicity between pH 5.8 (Fig. 5a) or pH 7.4 (Fig. 5c) and pH 6.5 (Fig. 5b), seems to be further intensified at higher temperatures. For instance, at an incubation temperature as high as 45C, the percent viabilities at pH 5.8 (Fig. 5a) and pH 7.4 (Fig. 5c) are around 60-65% and 55-60%, respectively; conversely, at pH 6.5 (Fig. 5b), viability decreases even further to around 40%. Thus, it appears that for pH 6.5 (Fig. 5b), cell viability decreases more rapidly with increases in incubation temperature, while at pH 5.8 (Fig. 5a) and pH 7.4 (Fig. 5c), this decrease is impeded, retaining higher viabilities.

Furthermore, data suggests that this characteristic increase in cytotoxicity with increase in temperature observed at pH 6.5 (Fig. 5b) culminates with percent viabilities (pH 6.5 at 45C) that approach cytotoxic levels found in Lipofectamine® (~40%; Fig. 5d). In contrast, both pH 5.8 (Fig. 5a) and pH 7.4 (Fig. 5c) maintain significantly higher cell survival than Lipofectamine® (Fig. 5d), independent of incubation temperature and time.

3.5 Gene Modulation Using SBF BA-GAPDH siRNA NPs

SBF BA-GAPDH siRNA particles were utilized to investigate gene regulation and quantify transfection efficiency as a function of incubation time, temperature, and nucleation pH. GAPDH, a common enzyme found in functional cells, is important for cellular metabolism. Therefore, a direct measurement of metabolic activity would illustrate the shifting behavior of a cell in response to a metabolic modulatory cue. Both positive and negative control GAPDH-siRNA sequences were consequently used to regulate and quantify gene knockdown. An increase in fluor over time, as mediated by horseradish peroxidase, was measured to evaluate relative

down-regulation of GAPDH enzyme for specified BA-NP synthesizing conditions. For example, at pH 6.5 comparing fluor increase for 37C positive and negative controls reveal large knockdown (lower values in fluor over time) for all incubation temperatures (Fig. 6a). Percent mean knockdown values were normalized to negative controls and compared against Lipofectamine® reaction conditions.

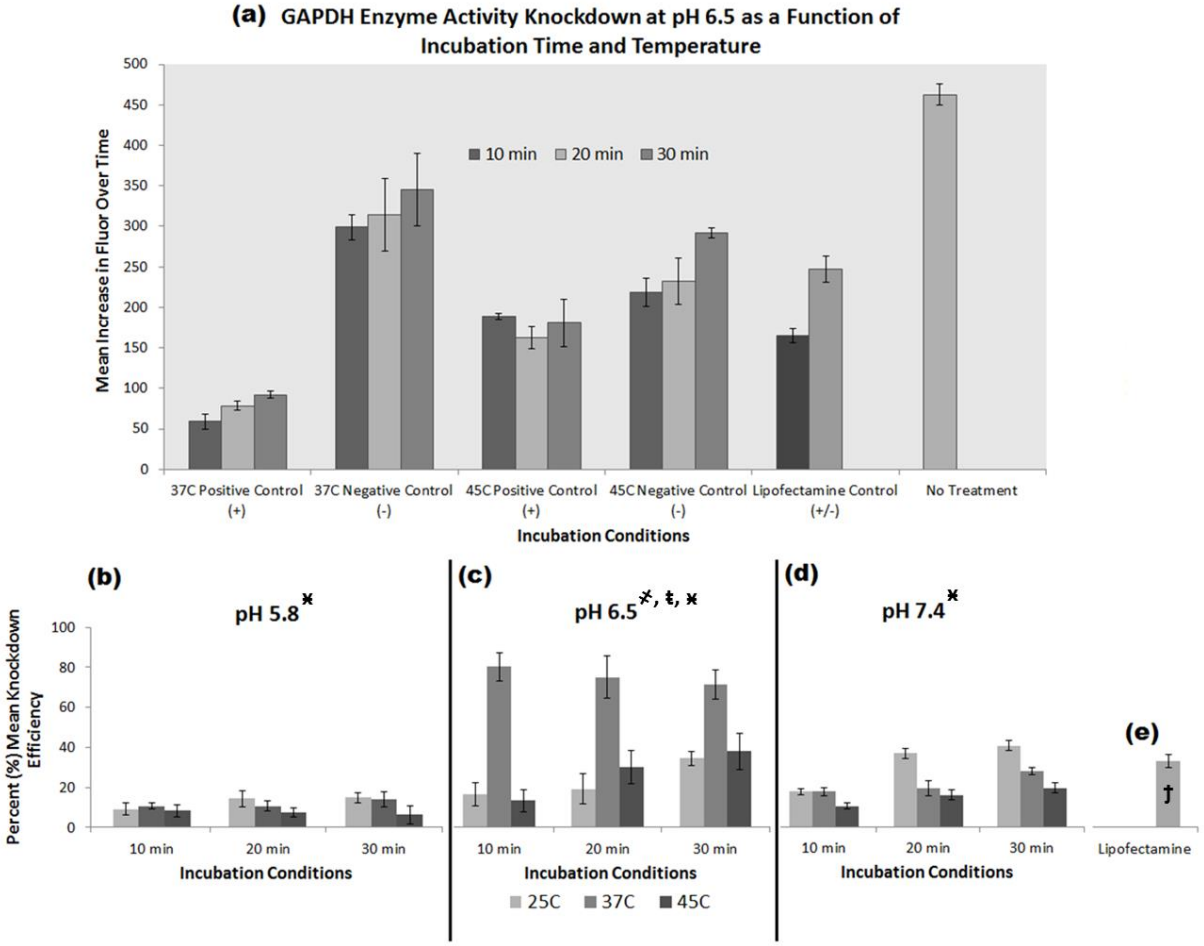

FIGURE 6. Quantitative gene modulation using a multitude of SBF BA-GAPDH-siRNA NPs. Large volumes of data depicting gene knockdown in comparison to negative and Lipofectamine® controls (a) can be collected for a singular pH as a function of incubation time and temperature. From this, percent mean knockdown efficiency values in relation to appropriate controls can be generated as is illustrated for pH 5.8 (b), pH 6.5 (c), and pH 7.4 (d). At pH 5.8 (b), an increase in incubation time (independent of temperature) causes negligible to minimal increase in knockdown. In contrast at pH 7.4 (d), as time increases, change in knockdown statistically increases for 25C, but remains statistically insignificant for 37C and 45C. SBF particles generated at pH 6.5 (c) shows maximized knockdown at 37C compared to other reaction conditions (b, d) and Lipofectamine® (e), and more accurately demonstrates a positive correlation in knockdown with increases in incubation time for 25C and 45C, regardless of temperature. *Statistical significance maintained:* ≠ *at given incubation times ($p<0.045$);* ŧ *among incubation temperatures ($p<0.043$);* ⁎ *between nucleation pH ($p<0.035$);* † *compared to pH 6.5-37C-30 min ($p<0.024$)*

For pH 5.8 (Fig. 6b), increases in incubation temperature produces negligible to minimal increases in transfection efficiencies (quantified as percent mean knockdown), whereas at pH 6.5 (Fig. 6c), incubation at 37C seems to produce statistically significant differences in gene knockdown. Specifically at pH 6.5 (Fig. 6c), both 25C and 45C incubation temperatures yield lower transfection efficiency with increase in time, in contrast to 37C where transfection efficiency values are higher and remain relatively unchanged with increase in time. At pH 7.4 (Fig. 6d), although increase in incubation time generally results in negligible to visible increases in transfection efficiency, for a specific time point, percent knockdown values for 37C are significantly lower than those observed at pH 6.5 (Fig. 6c) and discernibly higher than those measured at pH 5.8 (Fig. 6b), showing a notable reversion in data set to a state in-between pH 5.8 (Fig. 6b) and pH 6.5 (Fig. 6c). A similar propensity but to a lesser degree is detectable for 25C and 45C at pH 7.4 (Fig. 6d), with knockdown efficiency values generally being lower than pH 6.5 (Fig. 6c) but higher than pH 5.8 (Fig. 6b) for a given time.

Percent knockdown at pH 5.8 (Fig. 6b), when compared to that of Lipofectamine® (Fig. 6e), is statistically lower for all incubation time and temperatures; in contrast, at pH 6.5 (Fig. 6c) an increase in incubation time for 25C and 45C results in efficiency values approaching and surpassing Lipofectamine® (*e.g.* pH 6.5-25C-10 min vs. pH 6.5-25C-30 min; Fig. 6e). Although a parallel trend is noticeable for pH 7.4 (Fig. 6d) at 25C, both 37C and 45C reproduce characteristics observed at pH 5.8 (Fig. 6b) where percent knockdown is consistently below Lipofectamine® (Fig. 6e), independent of incubation time. Markedly, SBF BA-NP transfection efficiencies at pH 6.5 (Fig. 6c) and 37C are significantly larger than those of Lipofectamine® (Fig. 6e) control for all three time points.

3.6 Cellular Viability of SBF BA-GAPDH siRNA NPs at pH 6.5-37C

In order to assess any SBF BA-NP concentration dependence on cell viability, particles were produced at an optimal pH of 6.5 and incubation temperature of 37C, assayed using BCA, and compared against Lipofectamine® controls. Data proposes that with an increase in concentration of SBF BA-siRNA NPs (Fig. 7a), from 0.313 mM to 2.5 mM, the relative total protein expression remains consistently high at about 70-80%. In contrast, Lipofectamine®-siRNA NPs (Fig. 7b) ranging from 2 µL (manufacturer prescribed) to 3 µL, yielded cellular viabilities around 35-40%, suggesting that in efforts to further maximize transfection efficiency, a high concentration of SBF BA-NPs (~2.5 mM; Fig. 7a) synthesized at pH 6.5-37C and 30 min can be used without compromising cell viability.

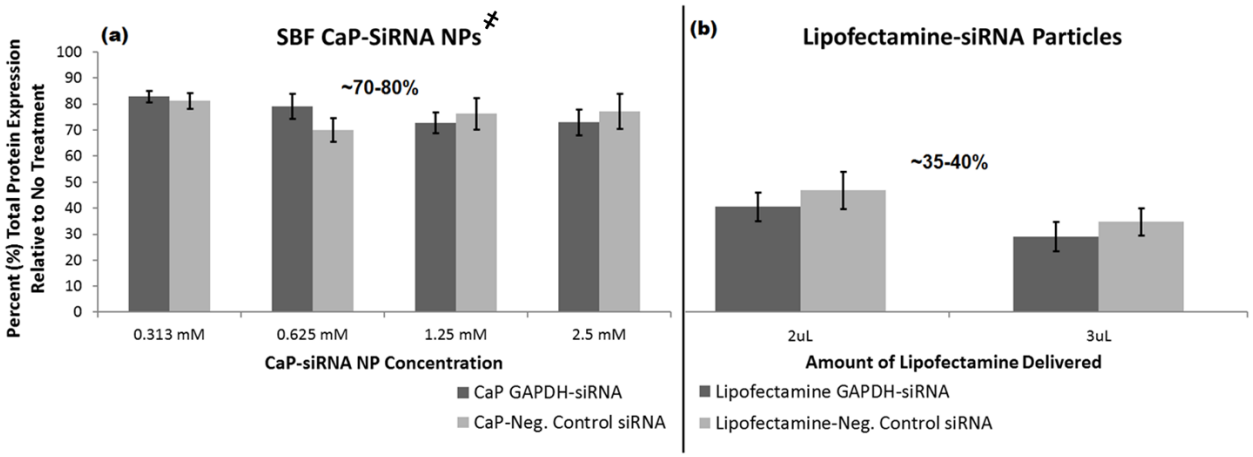

FIGURE 7. Cell viability of MC3T3 cells for various concentrations of SBF BA-siRNA particles fabricated at pH 6.5-37C-30 min. BA-NPs generated using established SBF protocol at an optimal state of pH 6.5-37-30 min provided ~70-80% cell viabilities (a), even at larger NP concentrations (2.5 mM), compared to Lipofectamine® doses (2-3 µL) that had statistically greater cytotoxicity (b). ** Statistical significance ($p<0.022$) maintained between Lipofectamine® amounts delivered*

3.7 Transfection using SBF BA-hsa miRNA NPs at pH 6.5-37C

Pre-miR hsa-miRNA, a common genetic sequence exploited to knockdown PTK-9 activity, was employed as means to establish and reveal the versatility of this NP delivery platform. Specifically, BA-miRNA NPs were synthesized using SBF at pH 6.5-37C for an incubation time of 30 min. Resulting particles were analyzed for morphological traits under SEM

at 20,000x (Fig. 8a), loaded with miRNA-FAM to assess cellular uptake (Fig. 8b), quantified for cellular viability at 2.5 mM BA-NP concentration (Fig. 8c-d), and evaluated for gene knockdown against Lipofectamine® (Fig. 8e).

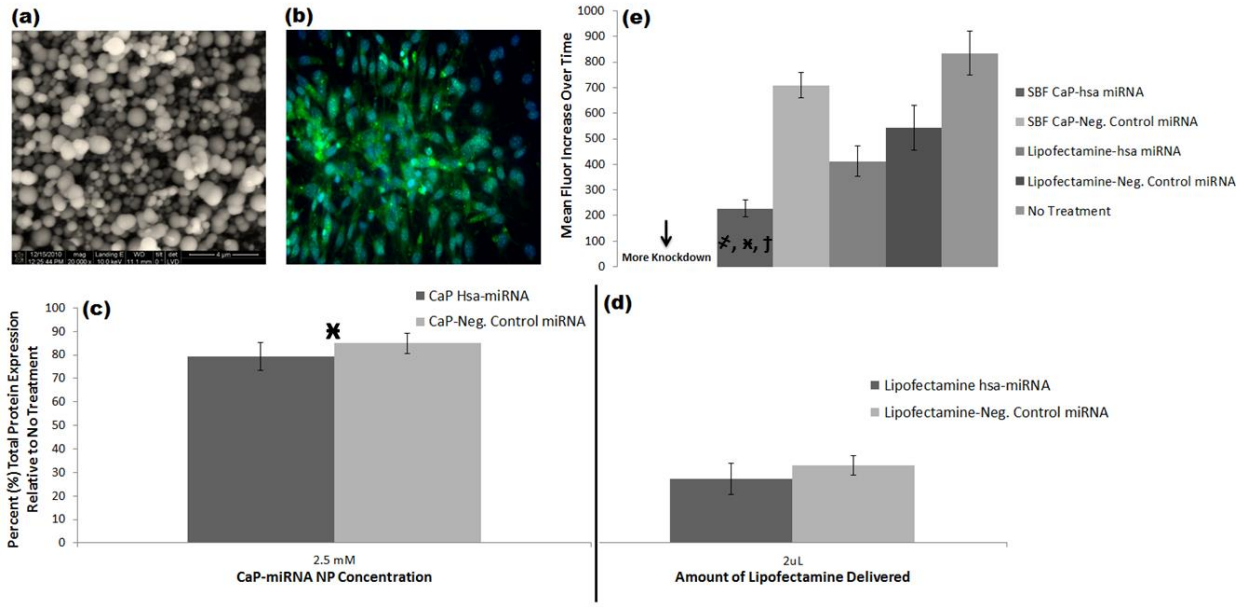

FIGURE 8. Synthesis and application of SBF BA-hsa-miRNA NPs for gene transfection at pH 6.5-37C-30 min. Hsa-miRNA sequences were loaded in CaP nanocarriers using the same SBF protocol as used for GAPDH-siRNA NPs. Scanning electron microscopy (a) describes the particles to have similar morphology (homogenous distribution of well nucleated particles) to those generated by SBF BA-siRNA at an equivalent reaction condition. Moreover, cell uptake (b) and viability (c-d) remains equally high in comparison to SBF BA-siRNA NPs; this is represented by distinct, non-nuclear cellular fluorescence and ~80-85% cell viability at a maximum BA-NP concentration. Furthermore, loss-of-function experiments (c) demonstrate a preservation of maximal knockdown of target protein compared to no treatment and Lipofectamine® controls. *Statistical significance maintained: $^{\neq}$between negative control –miRNA ($p<0.019$); $^{\varkappa}$among Lipofectamine® controls ($p<0.023$); †between no treatment ($p<0.014$)*

Qualitative SEM suggests BA-miRNA particles (Fig. 8a) of similar spheroidal morphology to BA-siRNA NPs (Fig. 2b) are generated under equivalent reaction conditions, with samples containing high concentrations of homogenously distributed NPs with limited aggregation around less prominent salt crystals. These BA-NPs, once prepared with miRNA-FAM at pH 6.5-37C (Fig. 8b), provides high uptake in MC3T3 cells (increased fluorescence) comparable to uptake of BA-siRNA FITC NPs (Fig. 3c). BCA assays conducted on cells grown in the presence of BA-hsa miRNA NPs (Fig. 8c) seem to indicate similar percent total protein expression (~80-85%) to that of BA-GAPDH siRNA NPs (Fig. 5b), suggesting high cellular

viabilities compared to traditional dosages of Lipofectamine® (Fig. 8d) and analogous to those discovered using BA-siRNA NPs (Fig. 5b). Lastly, gene modulation studies utilizing BA-hsa miRNA NPs fabricated at pH 6.5-37C and 30 min (Fig. 8e) appears to illustrate a larger knockdown (decreased fluor) of PTK-9 activity than Lipofectamine® control, matching and complimenting optimized data previously attained using BA-GAPDH siRNA NPs (Fig. 6c).

4. DISCUSSION

The preparation of SBF NPs is inherently sensitive [33-35], where particle nucleation and growth occurs vigorously; however, as results indicate, this system can be controlled by regulating key parameters. Variations in nucleation pH, incubation temperature, and incubation time seem to provide the basis for a tunable system with the capacity to create characteristic outcomes in gene modulation and cellular toxicity. These distinct results originate from the presence and subsequent manipulation of morphological and solution properties of SBF BA-NPs (Fig. 2a-d). Controlling nucleation and growth of particles in SBF by systematically decreasing temperature (Fig. 2b) or appropriately adjusting pH (Fig. 2d) can construct more ordered microenvironments where the NP-solution imposes a more favorable interaction with surrounding cells. In addition, understanding SBF solution qualities where regulating precipitation of salt crystals can also play a critical role in recognizing cellular viability. More specifically, data suggests that these types of reaction conditions, where NPs of similar size are synthesized and are more homogenously distributed (Fig. 2b), allow for lower cytotoxicity, as shown by an increase in cell viability at lower temperatures for a given pH (Fig. 5b). Aggressive forms of particle evolution, marked by the existence of large salt agglomerates and numerous NP clusters (Fig. 2a), may allow for a less conducive cellular interaction and, in contrast, increase cytotoxicity, as demonstrated by an increase in incubation temperature independent of pH (Fig. 5a-c).

Exhibiting cellular compatibility represented by a cell viability of ~70% or higher is an important attribute in gene delivery systems [32]. For a given nucleation pH and temperature since particle morphological properties do not vary considerably with changes in incubation time (Fig. 2b-c), fluctuations in cell viability remain statistically insignificant from 10 min to 30 min

(Fig. 5a-c). Thus, it is important to note that in the time scale for particle generation, where a smaller incubation time results in increased system efficiency, there is greater influence by temperature and pH on cell viability (Fig. 5a-c), since varying both parameters contribute to significant morphological changes over short periods of time (Fig. 2a, d). Increasing incubation time to beyond 30 min can be hypothesized to cause notable differences in SBF NP solution properties, and consequently cell viability and gene modulation. Hence having a faster incubation time can not only serve to prevent intrinsic aggressive nucleation and particle growth, but function to create a high-throughput platform.

SBF BA-NP growth and development is more chaotic and aggressive with increase in temperature (Fig. 2a), resulting in lower cellular viability from 25C to 45C, independent of nucleation pH (Fig. 5a-c). Nevertheless, it appears that at both pH 5.8 (Fig. 5a) and 7.4 (Fig. 5b), cells experience similar cytotoxicities at 25C and 37C whereas for 45C, percent viabilities tend to be larger for pH 5.8 (Fig. 5a) than pH 7.4 (Fig. 5b). This suggests that although nucleation pH plays a central role in controlling cellular viability, substantial increases in incubation temperature can transition to be a dominant influence on cytotoxicity, as SBF solutions at high temperatures undergo indiscriminate precipitation (Fig. 2a). In contrast, at pH 6.5 (Fig. 5b) this deviation in cell viability with increase in incubation temperature is more prominent, as small increases in temperature from 37C to 45C cause percent viabilities to drop from ~70-75% to ~40%. This signifies that the SBF system is specifically more sensitive to changes in incubation temperature at pH 6.5 (Fig. 5b) than pH 5.8 (Fig. 5a) or pH 7.4 (Fig. 5c). This sensitivity could arise from differences in SBF solution buffering capacity, where extreme nucleation pH, defined by the presence of large concentrations (relative) of H+ or OH- ions in solution, could serve to efficiently buffer the production of large, toxic, salt agglomerates at high incubation

temperatures (Fig. 2a). Such buffering ions can act to quench free floating salt-crystal precursors, thereby limiting the formation of large salt agglomerates and increasing cellular viability as shown at pH 5.8-45C (Fig. 5a) compared to pH 6.5-45C (Fig. 5b). In efforts to control cell viability at high temperatures, preparation of SBF solution and subsequent NP nucleation should take place at more acidic or basic environments than pH 6.5.

Traditional transfection reagents such as Lipofectamine® function as liposomal carriers and are vastly utilized as comparative platforms in gene delivery [1, 32]. According to acquired data, Lipofectamine® maintains a relative cell viability of ~40% (Fig. 5d). In comparison, only SBF BA-NPs synthesized at pH 6.5-45C (Fig. 5b) produce particles that are equally toxic to that of Lipofectamine® (Fig. 5d), while at the same pH, lowering the incubation temperature statistically increases cellular viability. Moreover, reaction conditions where more acidic or basic environments are exploited (Fig. 5a, d) cytotoxicity remains considerably higher than Lipofectamine® controls (Fig. 5d), indicating that the SBF system, in general, yields better biocompatibility for gene delivery than liposomal based formulations.

Cell uptake studies provide a qualitative backbone in understanding the behavior of SBF BA-NPs *in vitro*, and demonstrate a co-dependence on pH and temperature. Increase in incubation time from 10-30 min at pH 6.5 for 37C (Fig. 3a-c) illustrates minimal to negligible effect on cell uptake, as small fluctuations in time at this reaction condition seems to produce modest morphological disparities (Fig. 2b-c). Moreover, as incubation temperature increases beyond a threshold (Fig. 3f, i), cell uptake appears to decrease as fluorescence intensities diminish, correlating to the development of large NP clusters (Fig. 2a). These NP agglomerates are harder to internalize via endocytic means (Fig. 4c), and can be easily removed during culture and washed away during cell rinsing. Therefore at pH 5.8 (Fig. 3d-e), there is an initial increase

in uptake from 25C to 37C as suitable particle formation increases (Fig. 2b); however, from 37C to 45C (Fig. 3e-f), NP growth is too aggressive (Fig. 2a) causing a loss in efficiency as many of the generated particles are not accessible to cells. A similar phenomenon is observed at pH 7.4 (Fig. 3g-i) where at a constant incubation time of 30 min, increase in incubation temperature beyond 37C results in a decrease in cell uptake, caused primarily by chaotic nucleation and growth (Fig. 2a). In fact at 30 min and 37C, there appears to be greater cell uptake (distinct fluorescent signals) at pH 6.5 (Fig. 3c) than pH 5.8 (Fig. 3e) or pH 7.4 (Fig. 3h), both of which provide similar fluorescent signals. Hence, pH 6.5-37C (Fig. 3c) seems to offer a point of control for the SBF system, where NP fabrication is more regulated and uptake is maximized.

Gene modulation using GAPDH-siRNA sequences help to examine knockdown efficacy of SBF BA-NP system. Quantitative transfection can be assessed as a function of tunable parameters and compared against appropriate negative controls to calculate relative percent mean knockdown efficiencies (Fig. 6a). Data seems to suggest peaks in knockdown efficiencies at pH 6.5-37C (Fig. 6c), where values range from ~70-80% independent of incubation time. This correlates to initial observations during NP internalizations at pH 6.5-37C (Fig. 3a-c), where variations in incubation time provides negligible influence in cell uptake. Moreover, at this particular reaction condition, NP assembly in solution is less aggressive and more controlled (Fig. 2b), creating homogenous particles surrounded by smaller defined salt lattice constructs that are less toxic (Fig. 5b). Thus, this more stable microenvironment appears to not only maintain maximized transfection efficiency (Fig. 6c), but also does so without compromising cellular viability (>70%; Fig. 5b). Deviations from pH 6.5-37C to higher and lower temperatures (Fig. 6c) drastically reduces efficiency at a given incubation time, and demonstrates a trend reversion from incubation time independent to time dependent knockdown. Specifically, at pH

6.5-25C, the low temperature creates minimal NP precipitates, thereby maintaining a relatively compatible microenvironment that generates high cellular viability (Fig. 5b) but limits transfection efficiency (Fig. 6c). Transitioning to a higher temperature where final SBF NP solution properties are harsher (Fig. 2a), as indicated by large particle and salt agglomerates, provides both lower viability (Fig. 5b) and knockdown (Fig. 6c) than pH 6.5-37C. Varying nucleation pH from 6.5 also seems to create noticeable differences in gene modulation. At a more acidic pH (Fig. 6b), knockdown efficiencies at 37C are considerably lower with minimal noticeable dependence on incubation time. Due to an increased solution buffering capacity at pH values lower than pH 6.5, an increase in temperature to 45C results in increased viability (Fig. 5a) and decreased knockdown (Fig. 6b), as local H+ ions interfere with salt crystal and BA-NP precipitation (Fig. 2d). A similar phenomenon can be observed at pH values larger than pH 6.5, where local concentrations of OH- regulate SBF NP solution properties to increase viability (Fig. 5c) but decrease knockdown (Fig. 6d). Upon comparison to Lipofectamine® control (Fig. 6e), only pH 6.5-37C (Fig. 6c) seems to produce percent knockdown values that are consistently higher (maximized transfection). In contrast, at pH 5.8 (Fig. 6b) transfection efficiencies remain consistently lower than gene knockdown due to Lipofectamine® (Fig. 6e).

The criteria for optimization of SBF BA-NP system is centered on locating an ideal reaction condition that maximizes transfection efficiency without compromising cell viability. From this systematic study, where individual key parameters were varied to assess cell uptake, cytotoxicity and gene modulation, generating SBF NPs at pH 6.5-37C seems to provide a suitable balance between high transfection (~70-80%; Fig. 6c) and minimal toxicity (~70-75% viability; Fig. 5b). Modifying incubation temperature significantly alters viability and knockdown. For example, although at pH 6.5-25C cytotoxicity is minimal (Fig. 5b), there is poor

gene modulation which decreases transfection efficiency (Fig. 6c). Changing nucleation pH to either pH 5.8 or pH 7.4 may seem like a fitting possibility since data maintains temperature-dependent high cell viabilities (Fig 5a, c); however; transfection efficiencies are drastically lower (Fig. 6b, d), suggesting that the system at such reaction conditions will fail to produce adequate gene regulation. Incubation time, though not as dominant of a factor as nucleation pH or incubation temperature, can still be critical in affecting SBF -BA particle morphologies in solution (Fig. 2c), especially at longer time periods. Furthermore, since incubation time does not create a significant difference in either cytotoxicity (Fig. 5b) or gene modulation (Fig. 6c) at pH 6.5-37C, exploiting a shorter incubation time (<30 min) can consequently increase the platform's gene delivery efficiency at the optimized synthesis condition. Against Lipofectamine® control (Fig. 7b), SBF BA-NPs of different concentrations fabricated at pH 6.5-37C (Fig. 7a) promotes greater viability and knockdown efficiency, suggesting that NPs synthesized from this reaction condition also improves *overall* delivery efficacy. In fact, since an increase in concentration of BA-NPs from 0.3 mM to 2.5 mM produces negligible changes in cell viability (Fig. 7a), in essence final concentrations of particles delivered to cells could be increased to further maximize transfection (Fig. 6c) while still maintaining low cellular toxicity (Fig. 5b).

In efforts to elucidate the versatility of SBF BA-NP system, miRNA sequences were incorporated to assess morphology (Fig. 8a), cell uptake (Fig. 8b), cytotoxicity (Fig 8c-d), and gene modulation (Fig. 8e) at pH 6.5-37C-30 min. Structural analysis via SEM (Fig. 8a) indicates similar morphological properties as attained by employing siRNA (Fig. 2b), with homogenously distributed NPs surrounded by distinct smaller salt crystals. Cell uptake using fluorescently labeled miRNA-FAM (Fig. 8b) demonstrates characteristic uptake as acquired by BA-siRNA-FITC at pH 6.5-37C (Fig. 3c) with noticeable, definite fluorescence. Using 2.5 mM BA-hsa-

miRNA, cytotoxicity remains relatively low (Fig. 8c) compared to Lipofectamine® control (Fig. 8d), suggesting cellular viability does not get affected when transitioning to different types of nucleic acids (Fig. 5b). Lastly, with a decrease in target gene expression (Fig. 8e), implying high knockdown, SBF BA-hsa-miRNA maintains analogous transfection efficiency as SBF BA-GAPDH-siRNA at an optimized state (Fig. 6c). Therefore, this well characterized SBF-BA system can serve as the basis for an adaptable gene delivery vehicle, combining different types of nucleic acids enhanced to transfect with high efficiency and minimal toxicity under optimized reactive conditions.

5. CONCLUSION

The formation of SBF carbonated appetites and subsequent precipitations of BA-NPs are intrinsically sensitive to synthesizing conditions and are highly tunable [41, 42]. As results have suggested, small variations in reaction parameters such as in pH, temperature, or time can cause diverse outcomes in cell viability and gene transfection, stemming from fundamental morphological transformations of NPs in solution. Due to the susceptibility of SBF [43, 44], there have been limited studies that have strictly investigated the optimization of SBF derived BA-NPs. In fact, it seems to be more common to find investigators utilizing a single parameter to control and regulate SBF NP nucleation and development [39-43], and although some have examined the process as a whole (i.e. constructing apatite layers in response to various stimuli) [31, 34, 36, 44], few have applied the approach to enhancing gene delivery.

Therefore the significance and uniqueness of this study focuses on systematically manipulating fabrication environments to thoroughly understand the effects of key NP assembly factors on cellular interactions, and in doing so, elucidate towards an optimized platform that can retain high efficacy, independent of the genetic sequence used. Specifically, a favorable and maximized reaction condition at pH 6.5-37C is established by recognizing changes in features such as NP morphology, cytotoxicity, and gene modulation. At this augmented state, particles achieve encouraging nanostructures defined by controlled precipitation that elicit improved cell uptake, minimal to tolerable cell toxicity, and amplified gene knockdown. Moreover, these modulatory profiles and trends seem to be characteristic of the specific reaction condition and not affected by genetic cargo (e.g. transitioning from -siRNA to -miRNA), signifying the SBF system's overall versatility, and the optimized condition's efficacy, explicitly.

While the study examined three critical parameters of this tunable platform, future efforts will be geared towards exploring the effects of more subtle factors (i.e. the ratio of CaP present in BA-NPs) as means to further refine the optimized state [45]. It is also necessary to examine relative gene transfection efficacy of this optimized SBF BA-NP system in a head-to-head comparison against other CaP-NP platforms and possibly other alternative non-viral vectors. Due to SBF's innate susceptibility, the polydispersity of BA-NPs tends to be high, and thus necessitates further modification of the SBF protocol by tweaking relative bulk concentrations of buffer salt ions in order to diminish screening of electric potential and prevent aggregation without altering the system's favorable transfection and bioactive properties. The addition of greater positively charged moieties on BA-NPs may also assist in the formation of more monodispersed particles, which can consequently be stabilized in solution through improved electrostatic repulsions. Furthermore, in order to appreciate the direct involvement of nucleic acid delivery in cancer therapy or tissue engineering applications, this enhanced SBF BA-NP system can be incorporated with relevant genes, from specific siRNA to pDNA [32], to assess transfection efficiency in therapeutic modalities. Ultimately, as numerous creative non-viral vectors, each with specific advantageous, emerge and receive more interest in gene therapy, a versatile and adaptable delivery system that can ensure high efficacy while limiting production time and cost will set the stage for the next generation nanomedicines.

6. REFERENCES

1. Nouri A, Castro R, Santos JL, Fernandes C, Rodrigues J, Tomas H (2012) Calcium phosphate-mediated gene delivery using simulated body fluid (SBF). **Int J Pharm** 434:199-208

2. Santos JL, Pandita D, Rodrigues J, Pego AP, Granja PL, Tomas H (2011) Non-viral gene delivery to mesenchymal stem cells: methods, strategies and application in bone tissue engineering and regeneration. **Curr Gene Ther** 11:46-57

3. Orrantia E, Chang PL (1990) Intracellular distribution of DNA internalized through calcium phosphate precipitation. **Exp Cell Res** 190:170-174

4. Seelos C (1997) A critical parameter determining the aging of DNA-calcium-phosphate precipitates. **Anal Biochem** 245:109-111

5. Jordan M, Wurm FM (2004) Transfection of adherent and suspended cells by calcium phosphate. **Methods** 33:136-143

6. Chou YF, Chiou WA, Xu Y, Dunn JCY, Wu BM (2004) The effect of pH on the structural evolution of accelerated biomimetic apatite. **Biomaterials** 25:5323-5331

7. Ma H, Diamond SL (2001) Nonviral gene therapy and its delivery systems. **Curr Pharm Biotechnol** 2:1-17

8. Luo D, Saltzman WM (2000) Synthetic DNA delivery systems. **Nat Biotechnol** 18:33-37

9. Smedt SC, Demeester J, Hennink WE (2000) Cationic polymer based gene delivery systems. **Pharm Res** 17:113-126

10. Behr JP (1994) Gene transfer with synthetic cationic amphiphiles: prospects for gene therapy. **Bioconjug Chem** 5:382-389

11. Dufes C, Uchegbu IF, Schatzlein AG (2005) Dendrimers in gene delivery. **Adv Drug Deliv Rev** 57:2177-2202

12. Tang MX, Redemann CT, Szoka FC (1996) In vitro gene delivery by degraded polyamidoamine dendrimers. **Bioconjug Chem** 7:703-714

13. Meredith A, Simanek M, Simanek E (2009) Non-viral vectors for gene delivery. **Chem Rev** 109:259-302

14. Li S, Huang L (2000) No-nviral gene therapy: promises and challenges. **Gene Ther** 7:31-34

15. Lev H, Zhang S, Wang B, Cui S, Yan J (2006) Toxicity of cationic lipids and cationic polymers in gene delivery. **J Control Release** 114:100-109

16. Thomas M, Klibanov AM (2003) Non-viral gene therapy: polycation-mediated DNA delivery. **Appl Microbiol Biotechnol** 62:27-34

17. Roy I, Mitra S, Maitra A, Mozumadar S (2003) Calcium phosphate nanoparticles as novel non-viral vectors for targeted gene delivery. **Int J Pharm** 250: 25-33

18. Graham FL, Van Der Eb AJ (1973) A new technique for the assay of infectivity of human adenovirus 5 DNA. **Virology** 52:456-467

19. Chowdhury EH, Akaike T (2007) High performance DNA nano-carriers of carbonate apatite: multiple factors in regulation of particle synthesis and transfection efficiency. **Int J Nanomedicine** 2:101-106

20. Bisht S, Bhakta G, Mitra S, Maitra A (2005) pDNA loaded calcium phosphate nanoparticles: highly efficient non-viral vector for gene delivery. **Int J Pharm** 288:157-168

21. Welzel T, Radtke I, Meyer-Zaika W, Heumann R, Epple M (2004) Transfection of cells with custom-made calcium phosphate nanoparticles coated with DNA. **J Mater Chem** 14:2213-2217

22. Sokolova V, Radtke I, Heumann R, Epple M (2006) Effective transfection of cells with multi-shell calcium phosphate-DNA nanoparticles. **Biomaterials** 27:3147-3153

23. Cheng PT, Pritzker KPH (1983) Solution Ca/P ratio affects calcium phosphate crystal phases. **Calcif Tissue Int** 35:596-601

24. Kokubo T, Kushitani H, Sakka S, Kitsugi T, Yamamuro T (1990) Solutions able to reproduce in vivo surface-structure changes in bioactive glass-ceramic A-W3. **J Biomed Mater Res** 24:721-734

25. Kokubo T, Takadama H (2007) Simulated body fluid (SBF) as a standard tool to test the bioactivity of implants. In: Epple M, Baeuerlein E, (Eds) *Handbooks of Biomineralization: Medical and Clinical Aspects*. Wiley-VCH, Weinheim, pp-97-108

26. Li P (2003) Biomimetic nano-apatite coating capable of promoting bone ingrowth. **J Biomed Mater Res** 66:79-85

27. Tanahashi M, Yao T, Kokubo T, Minoda M, Miyamoto T, Nakamura T, Yamamuro T (1994) Apatite coating on organic polymers by a biomimetic process. **J Am Ceram Soc** 77:2805-2808

28. Chen XB, Nouri A, Li YC, Lin JG, Hodgson PD, Wen CE (2008) Effect of surface roughness of Ti, Zr, and TiZr on apatite precipitation from simulated body fluid. **Biotechnol Bioeng** 101:377-387

29. Tsang EJ, Arakawa CK, Zuk PA, Wu BM (2011) Osteoblast interactions within a biomimetic apatite microenvironment. **Ann Biomed Eng** 39:1186-1200

30. Miyaji F, Kim HM, Handa S, Kokubo T, Nakamura T (1999) Bonelike apatite coating on organic polymers: novel nucleation process using sodium silicate solution. **Biomaterials** 20:913-919

31. Zhang R, Ma PX (1999) Porous poly(ι-lactic acid)/apatite composites created by biomimetic process. **J Biomed Mater Res** 45:285-93

32. Chowdhury E, Kunou M, Nagaoka M, kundu AK, Hoshiba T, Akaike T (2004) High-effeciency gene delivery for expression in mammalian cells by nanoprecipitates of Ca-Mg phosphate. **Gene** 341:77-82

33. Marques P, Serro AP, Sarmago BJ, Fernandes AC, Magalhaes M, Correia RN (2003) Mineralization of two calcium phosphate ceramics in biological model fluids. **J Mater Chem** 13:1484-1490

34. Yan WQ, Nakamura T, Kawanabe K, Nishigochi S, Oka M, Kokubo T (1997) Apatite layer-coated titanium for sue as bone bonding implants. **Biomaterials** 18:1185-1190

35. Wulur IH (2002) Microstructural control of biomimetically grown bonelike minerals on two dimensional and three dimenstional polymer surfaces. *M.S. thesis, Dept. of Bioengineering*, UCLA.

36. Uchida M, Hyun-Min K, Kokubo T, Miyaji F, Nakamura T (2001) Bonelike apatite formation induced on zirconia gel in a simulated body fluid and its modified solutions. **J Am Ceram Soc** 84:2041-2044

37. Li P, Ohtsuki C, Kokubo T, Nakanishi K, Soga N, Nakamura T, Yamamuro T (1992) Apatite formation induced by silica gel in a simulated body fluid. **J Am Ceram Soc** 75:2094-2097

38. Ohtsuki C, Kokubo T, Yamamuro T (1992) Mechanism of apatite formation on CaO SiO2 P2O5 glasses in a simulated boy fluid. **J Non-Cryst Solids** 143:84-92

39. Aza P, Guitian F, Merlos A, Lora-Tamayo E, Aza S (1996) Bioceramics – simulated body fluid interfaces: pH and its influence of hydroxyapatite formation. **J Mater Sci** 7:399-402

40. Jianguo L, Hailhong L, Malena S (1997) Characterization of calcium phosphates precipitated from simulated body fluid of different buffering capacities. **Biomaterials** 18:743-747

41. Barrere F, Blitterswijk CA, Grook K, Layrolle P (2002) Influence of ionic strength and carbonate on the Ca-P coating formation from SBF x 5 solution. **Biomaterials** 23:1921-1930

42. Barrere F, Blitterswijk CA, Groot K, Layrolle P (2002) Nucleation of biomimetic Ca-P coatings on Ti6A14 V from a SBF x 5 solution: influence of magnesium. **Biomaterials** 23:2211-2220

43. Seiji B, Maruno S (1995) Effect of temperature on electrochemical deposition of calcium phosphate coatings in a simulated body fluid. **Biomaterials** 16:977-981

44. Lu X, Leng Y (2005) Theoretical analysis of calcium phosphate precipitation in simulated body fluid. **Biomaterials** 26:1097-1108

45. Ferraz MP, Monteiro FJ, Manuel CM (2001) Hydroxyapatite nanoparticles: a review of preparation methodologies. **J Appl Biomater Biom** 2:74-80